Asian Journal of Green Chemistry 5 (2021) 135-150

Asian Journal of Green Chemistry

Journal homepage: www.ajgreenchem.com

Original Research Article

Green synthesis of silver nanoparticles from *Citrus sinensis* peel extract and its antibacterial potential

Kamrun Nahar[a], Md. Hafezur Rahaman[a], G.M. Arifuzzaman Khan[a], Md. Khairul Islam[b], Sharif Md. Al-Reza[a,*]

[a] *Department of Applied Chemistry and Chemical Engineering, Islamic University, Kushtia 7003, Bangladesh*

[b] *Department of Electrical and Electronic Engineering, Islamic University, Kushtia 7003, Bangladesh*

ARTICLE INFORMATION

Received: 2 June 2020
Received in revised: 6 August 2020
Accepted: 12 August 2020
Available online: 12 September 2020

DOI: 10.22034/ajgc.2021.113966

KEYWORDS

Green synthesis
Silver nanoparticles
Citrus sinensis
Spectroscopic analysis
Antibacterial activity

ABSTRACT

In this research study, we reported a convenient and environmentally friendly method for the green synthesis of silver nanoparticles using *Citrus sinensis* (navel orange) peel. The synthesized silver nanoparticles were identified by colour change from colourless to dark brown due to surface plasmon resonance. The optimal synthesis condition for the AgNPs was determined by varifying different parameters such as peel extract concentration, temperature, $AgNO_3$ concentration, effect of ratio of peel extract to $AgNO_3$ solution, pH and reaction time. The synthesized nanoparticles were identified using the UV-vis spectrophotometer, transmission electron microscopy (TEM), scanning electron microscopy (SEM), and dynamic light scattering (DLS) techniques. The qualitative phytochemical analysis of peel extract was performed to determine the presence of the alkaloids, phenolics, flavonoids, carbohydrates, saponins, triterpenes and tannins. The presence of the phytochemicals were also confirmed by FT-IR spectroscopy analysis. The synthesized silver nanoparticle also revealed good antibacterial activity against some important bacteria *Bacillus subtilis*, *Pseudomonas aeruginosa, Staphylococcus aureus* and *Escherichia coli*.

© 2021 by SPC (Sami Publishing Company), Asian Journal of Green Chemistry, Reproduction is permitted for noncommercial purposes.

Corresponding author, email: sharif@acce.iu.ac.bd (S.M. Al-Reza).
Tel.: +880 1911777183; Fax: +880 7174905.

Graphical Abstract

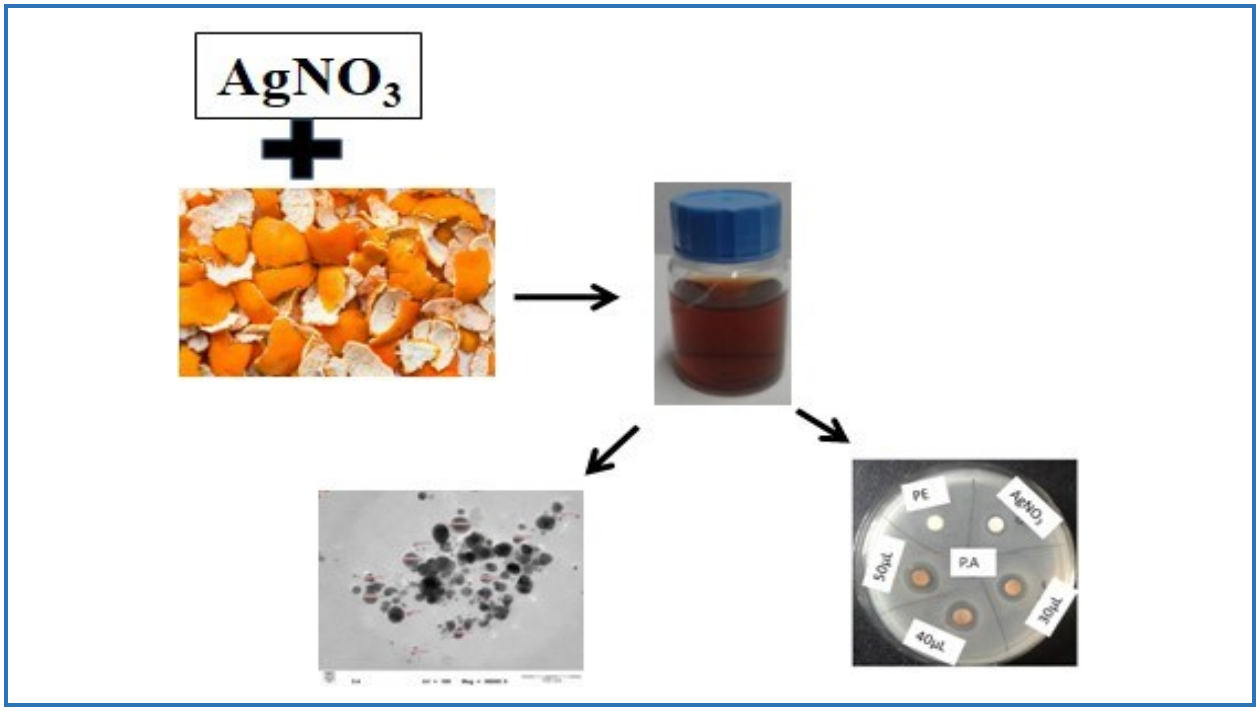

Introduction

Nowadays, there is an emerging interest in the synthesis of nanomaterials due to their properties that are not found in bulk. The behavior of nanomaterials is highly dependent on the shape and size of nanoparticles, which is a key factor in the use of nanoparticles [1]. Among several nanoparticles, silver nanoparticles have received a great deal of attention due to their unique physical and chemical properties in electro analytical, electrochemical, and bio-electrochemical applications [2].

There are various approaches for the synthesis of Ag-NPs, including physical and chemical methods such as micro-emulsion, polyol process, microwave assisted process and reduction through chemical, electrochemical, radiation and photochemical methods. However, these methods usually involve disadvantages such as high cost, toxic, tedious work-up and non-eco-friendly performance with high exhaustion of energy and time [3].

Moreover, the development of efficient green-chemistry procedures for the synthesis of metal nanoparticles has become a major focus of researchers. One of the most observed techniques is the synthesis of metal nanoparticles using the organisms. Among these, plants are the most feasible candidates as they are pertinent for huge amount biosynthesis of nanoparticles. These approaches have many advantages over the chemical and microbial synthesis as there is no complicated process for culturing and maintaining the cell, using hazardous chemicals, high-energy and wasteful purifications [4].

Recently, as a further step towards the development of greener and more sustainable processes, attempts have been made to replace plant parts with agroindustrial wastes [5]. Citrus fruits are mostly ingested as fresh prepare juice all over the world and the peel throw away as waste which contains large amount of secondary metabolites with potential antioxidant activity in comparison with other portions of the fruit [6]. In addition, it provides a sample supply of vitamin C, potassium, pectin and folic acid [7]. These citrus fruit residues, which are generally discarded as waste can be a good source of nutrition. The usage of these bioactive citrus residues can give an eco-friendly and low cost platform for the synthesis of novel nanoparticles.

There are few reports to date on the green synthesis of various nanoparticles such as gold nanoparticles [8], zinc oxide nanoparticles [9] and silver nanoparticles [10] from *Citrus sinensis* peel extract have been published.

However, there is no report available on the synthesis of silver nanoparticles from *Citrus sinensis* peel extract in Bangladesh. For the first time, we synthesized silver nanoparticles from aqueous extract of *Citrus sinensis* peel by reducing the silver ions present in the silver nitrate solution. The characterization was carried out using different spectroscopic analysis. The synthesized silver nanoparticles were also tested for antibacterial activity.

Experimental

Preparation of plant extract

Citrus sinensis fruits were bought from the local market in Kushtia, Bangladesh. The peel of *Citrus sinensis* was rinsed with distilled water to clean the dust. Then it was sundried to remove the residual moisture. The peel was homogenized to fine powder using an electric blender. 2 g of powder samples were boiled in 100 mL deionized water for 10 min at 80 °C. Then cool and filtered the aqueous peel extract through Whatman No. 1 filter paper. The filtered extract was kept in refrigerator at 4 °C for further experiment.

Synthesis of silver nanoparticle

An aqueous solution of 80 mL 0.01 M $AgNO_3$ was added to 20 mL of peel extract and the mixture was stirred with a magnetic stirrer at 25 °C and 60 °C, respectively. The solution colour was changed from the colourless to dark brown. Formation of the silver nanoparticles was primarily identified by colour change. The silver nanoparticles were separated from the solution by centrifugation after that AgNPs were washed with distilled water and acetone to discard water soluble particles. Finally, the nanoparticles were lyophilized and stored for characterization.

Standardization

For cost-effective production of silver nanoparticles, effect of concentration of peel extract, reaction time, temperature, pH, ratio of peel extract to $AgNO_3$ solution and concentration of $AgNO_3$ on AgNPs formation were investigated and the optimum conditions for the reaction were selected.

Characterization of silver nanoparticles

Silver nanoparticle was characterized by visual observation and spectroscopic methods. In visual observation, color change of the solution was confirmed by naked eye. AgNPs in solution was identified by using UV-visible spectrometer (Shimadzu UV-visible 2900 spectrometer) in the wavelength (λ) range 300-600 nm. Surface chemistry of AgNPs and biomolecules in *C. sinensis* extract were characterized by using Fourier transform infrared spectroscopy (Shimadzu FTIR spectrophotometer, FTIR 8400 Shimadzu, Japan). The FTIR spectra were recorded from 4000-600 cm^{-1}. Transmission electron microscopy (TEM) (Jenama/model: philip/ TEM CM12, Malaysia) was used to determine the particle size and surface morphology of nanoparticles. The shape, size and surface of synthesized AgNPs were analyzed by scanning electron microscope (JSM- 6490, JEOL C0, Ltd., Japan) with high-resolution images and selected area. The phase distribution, purity and crystallinity of the synthesized nanoparticles was confirmed by X-ray diffraction (XRD) (D8-Advance, Bruker, Germany). Dynamic light scattering (DLS) (Malvern, UK) studies justified the size of nanoparticles in the colloidal system without any aggregation and the hydrodynamic size.

Photochemical screening

The qualitative phytochemical analysis of *C. sinensis* extract was carried out to determine the presence of flavonoids (alkaline reagent), alkaloids (Dragendorff's), tannins (Few $FeCl_3$), phenolics (lead acetate, alkaline reagent test), saponins (foam test), triterpenes (Liberman test) and carbohydrates (Molish test) [11–13].

Antibacterial activity assay

The antibacterial activity was determined by agar disc diffusion method [14] using 100 µL of standardized inoculums suspension containing 10^7 CFU/mL of bacteria. Two gram-positive (*Bacillus subtilis* and *Staphylococcus aureus)* and two gram-negative (*Escherichia coli* and *Pseudomonas aeruginosa)* bacteria were used in this study. They were collected from the department of applied nutrition and food technology, islamic university, Kushtia, Bangladesh. After weighing the dried AgNPs were dispersed in deionized water to produce a stock solution with final concentration of 10 µg/µL. The tested samples were poured into each sterilized filter paper discs (6 mm diameter) using

micropipette. Tetracycline (Sigma-Aldrich Co., St. Louis, MO, USA) was used as standard reference antibiotics for this experiment. The plates were incubated at 37 °C for 24 h. The diameter of the inhibition zones was measured for the evaluation of antibacterial activity against the tested bacteria.

Results and Discussion

Visual observations

The formation of silver nanoparticles was primarily identified by colour change. Visually *Citrus sinensis* peel extract was mixed with 0.01 M silver nitrate solution showed a colour change from colourless to light yellow within 90 min (Figure 1b) then the colour changes from light yellow to brown (Figure 1c) and finally it was turned to dark brown after 210 min at 25 °C (Figure 1d). The color intensity increased with time of incubation as well as the yellow coloured solution coverted to dark brown within 210 min which may be due to the increased concentration of nanoparticles and the surface plasmon resonance in the aqueous solution [15, 16]. Finally no further color change of the solution was shown after 24 hrs (Figure 1e).

Standardization

Some parameters were optimized for the efficient formation of silver nanoparticles.

Concentration of C. sinensis peel extract

There was a difference in the formation of AgNPs by increasing the concentration of peel extract (Figure 2). Different concentrations of *C. sinensis* peel extract (20 g/L, 40 g/L, 60 g/L and 80 g/L) were utilized for the maximum production of AgNPs and the absorbance peak becomes more narrow and intense with the increasing of concentration. The absorption intensity increases monotonically with increasing concentration of peel extract. The highest absorption peak was observed when using 80 g/L *C. sinensis* peel extract.

Reaction time

The UV-vis spectra of the mixture was recorded at different time interval (60 min - 270 min) to optimize the reaction time. It can be inferred that at between 90 min and 120 min the surface plasmon resonance band is broadened due to slow transformation of Ag^{+} to Ag^{0} nanoparticles. Plasmon band formation increases with the increase of the reaction time due to large amount of Ag^{+} has been converted to Ag^{0}. The maximum absorption in the UV-vis spectra confirm the maximum production of nanoparticles. A broad peak and increasing absorbance were observed at 210 min with wavelength 442 nm (Figure 3). However, further increase in reaction time shows remarkable

decrease in absorption intensity and wavelength which is an evidence of some aggregation of silver nanoparticles [17].

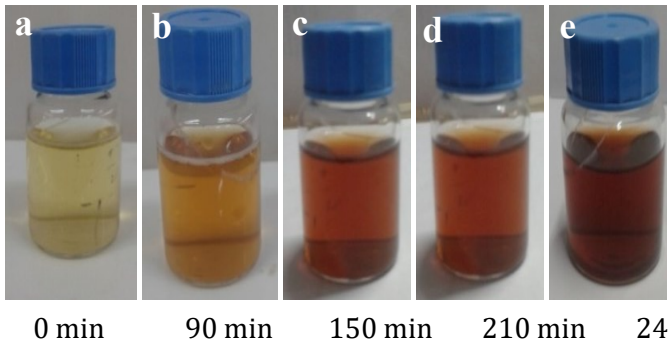

Figure 1. Color change at different time interval of *Citrus sinensis* peel extract solution with 0.01 M $AgNO_3$ solution, a) 0 min, b) 90 min, c) 150 min, d) 210 min, e) 24 hrs

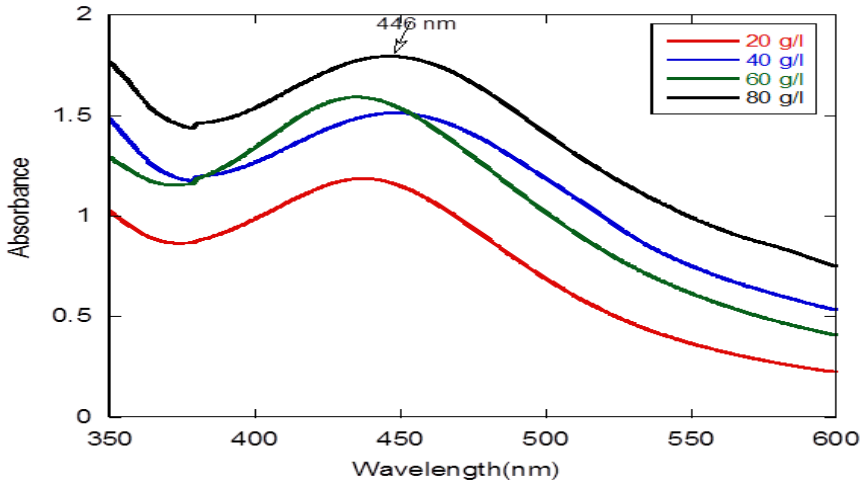

Figure 2. UV-vis absorbance spectra of silver nanoparticles synthesis by different concentration of *C. sinensis* peel extract

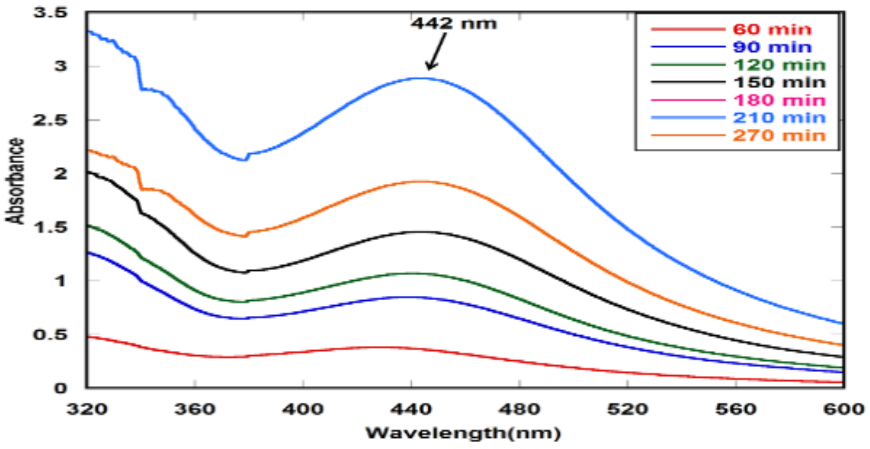

Figure 3. UV-vis absorbance spectra of silver nanoparticles synthesis by peel extract of *C. sinensis* at different reaction time

Temperature

Temperature is an important factor since it controls the nucleation process of nanoparticles configuration. The temperature of the reduction reaction was maintained at 30 °C, 40 °C, 50 °C, 60 °C, 70 °C and 80 °C and the absorbance of the resulting solution was measured spectrophotometrically. Figure 4 shows that the AgNPs formation start at 30 °C and maximum absorbance observed at 60 °C. An increase in the production of AgNPs was found when the temperature of the reaction was increased up to 60 °C, though beyond this there was a fall in absorbance.

Concentration of silver nitrate solution

In this study different concentrations of $AgNO_3$ solution (0.002 M, 0.004 M, 0.006 M, 0.008 M, 0.01 M and 0.015 M) were utilized in order to maximize the yield to AgNPs. The peak intensity raised with the increase in silver nitrate concentration from 0.002 M to 0.01 M indicating faster rate of bioreduction with increased concentration of parent salt [18]. But further increase in silver nitrate concentration to 0.015 M lead to lower peak intensity which can be adjudged by the formation of agglomerated nanoparticles and their settling. The UV-visible absorption spectra showed high absorbance peak intensity when the concentration of $AgNO_3$ solution was 0.01 M (Figure 5).

Ratio of peel extract and silver nitrate solution

Figure 6 reveals the ratios of *C. sinensis* peel extract and silver precursor in the ranges of 1:1, 1:2, 1:3, 1:4, 2:3, 3:5 and 4:5 were utilized in order to find out the optimum composition for the preparation of AgNPs. We found that the optimum composition of *C. sinensis* extract and silver nitrate solution in the reaction mixture was 1:2 to get maximum yield of AgNPs.

Effect of pH

Research work involves the issue on biosynthesis of nanoparticles at different pH (2, 5, 7, 9, and 11). At low pH (pH 2), no silver nanoparticles are formed. As the pH raises from 2 to 11, the absorption maximum shifts from 447 nm to 406 nm. The lower pH suppresses the nanoparticles formation due to low availability of functional groups of peel extract. Narrow absorption was shown at pH 7, 9 and 11. However, the large number of functional groups available for silver binding at higher pH and subsequently form a large amount of nanoparticles with smaller diameters. This indicates that pH 11 is the most favorable pH for the synthesis of AgNPs using *C. sinensis* peel extract (Figure 7).

Characterization

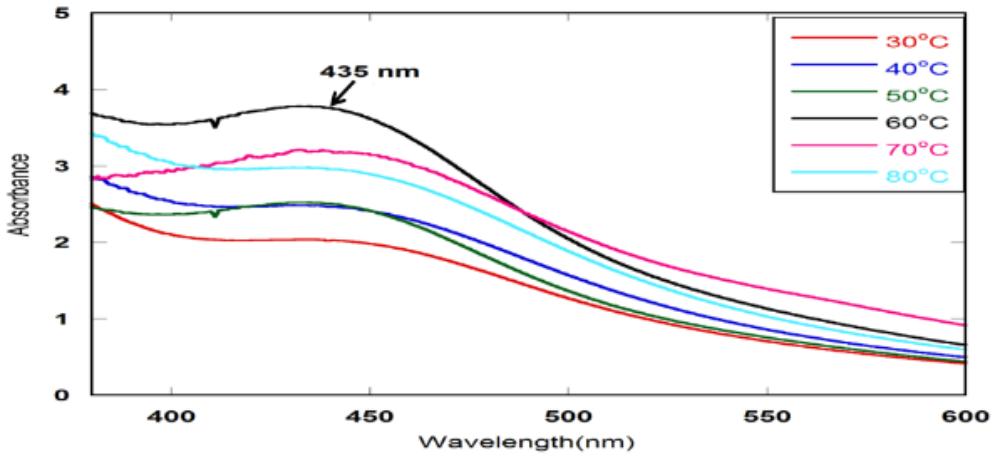

Figure 4. UV-vis absorbance spectra of silver nanoparticles from *C. sinensis* peel extract at different temperature

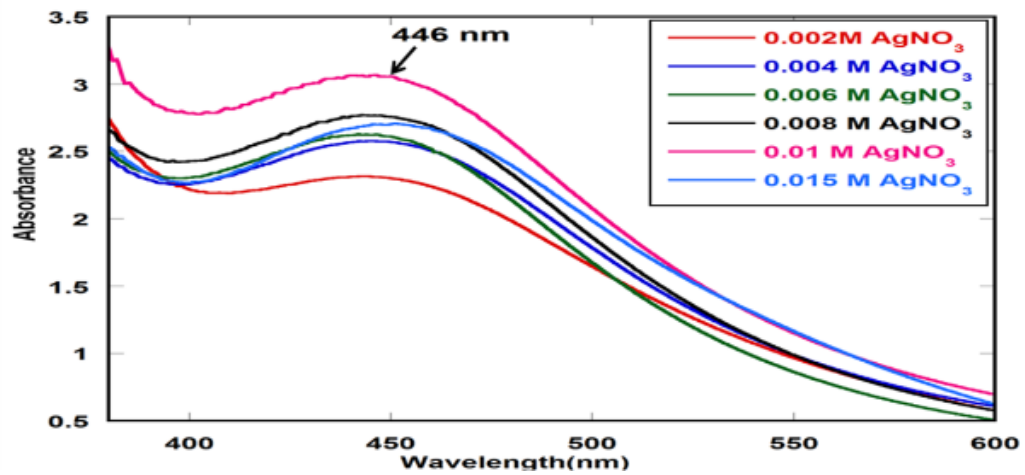

Figure 5. UV-vis absorbance spectra of *C. sinensis* AgNPs at different concentration of $AgNO_3$ solution

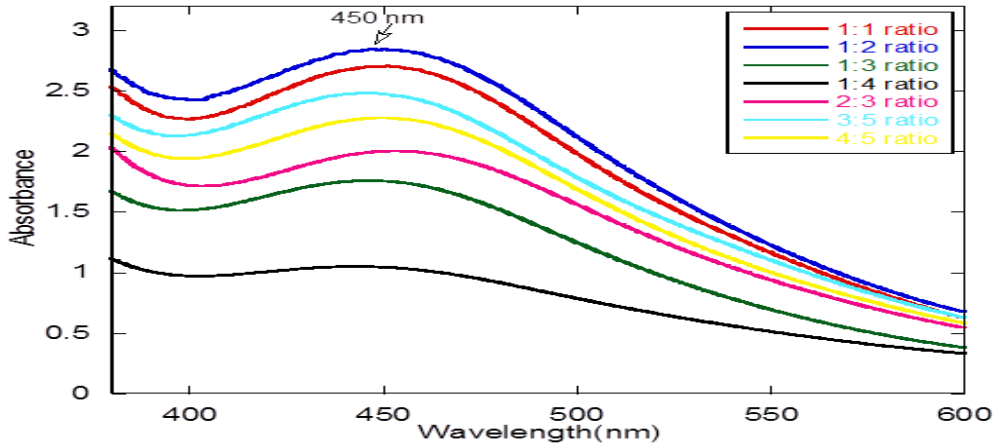

Figure 6. UV-vis absorbance spectra of AgNPs obtained from different ratios of *C. sinensis* peel extract and silver nitrate solution

UV-visible absorption spectrum

UV-vis spectroscopy is the primary method to identify the presence of AgNPs through green synthesis [19]. The synthesized nanoparticles exhibit dark brown color because of the excitation of surface plasmon resonance in AgNPs. In particular, absorbance in the range of 400 nm to 450 nm has been operated as an indicator to identify the reduction of Ag^{+} to metallic Ag^{0}. An broad absorbance peak at around 444 nm confirmed the reduction of $AgNO_3$ into nanoparticles (Figure 8). A broad peak centered around 400 nm is the characteristic surface plasmon resonance absorption of spherical silver nanoparticles. The broadness of the band is due to the wide sizes of the nanoparticles [20].

Fourier transform Infra-red

Fourier transform infrared is very important tool to identify the attachment of functional groups in between metal particles and biomolecules which is used to search the chemical composition of the surface of the nanoparticles and recognize the biomolecules for capping and effective stabilization of nanoparticles [21]. As shown in Figure 9, FTIR spectrum of *C. sinensis* peel extract shows major peak positions at 3444, 2927, 2856, 1635, 1118 and 742 cm^{-1}. On the other hand, FTIR spectrum of synthesized nanoparticles shows major peak positions at 3446, 2074, 1638 and 739 cm^{-1}. The broad and intense peak at 3446 cm^{-1} corresponds to OH stretching vibrations of phenol/carboxylic group present in extract, a peak at 2074 cm^{-1} can be assigned to alkyne group present in phyto-constituents of extract. The peak found at 1638 cm^{-1} could be indicated to C=O stretching or amide bending [22]. The peak at 739 cm^{-1} assigned to C–H alkenes stretch. The observed peaks were mainly attributed due to presence of some secondary metabolites like flavonoids, triterpenes, tannins, steroids and saponins excessively present in plants extract (Table 1) as also suggested by other researchers [23, 24].

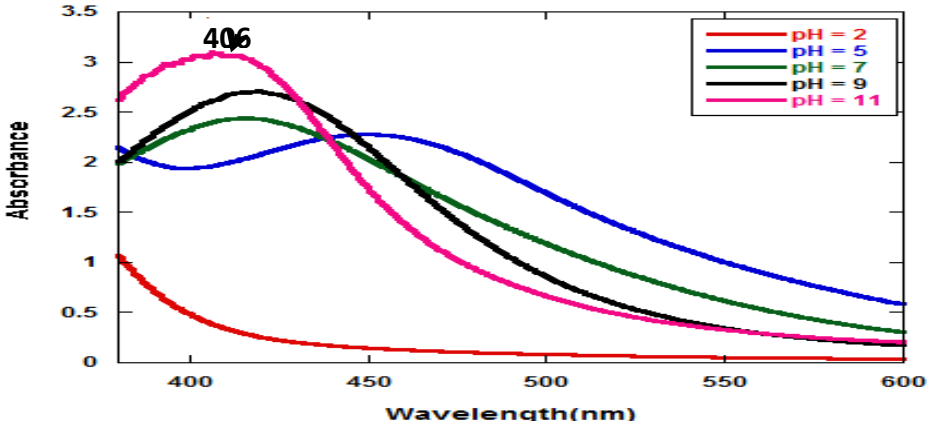

Figure 7. UV-vis absorbance spectra of AgNPs from *C. sinensis* peel extract at different pH

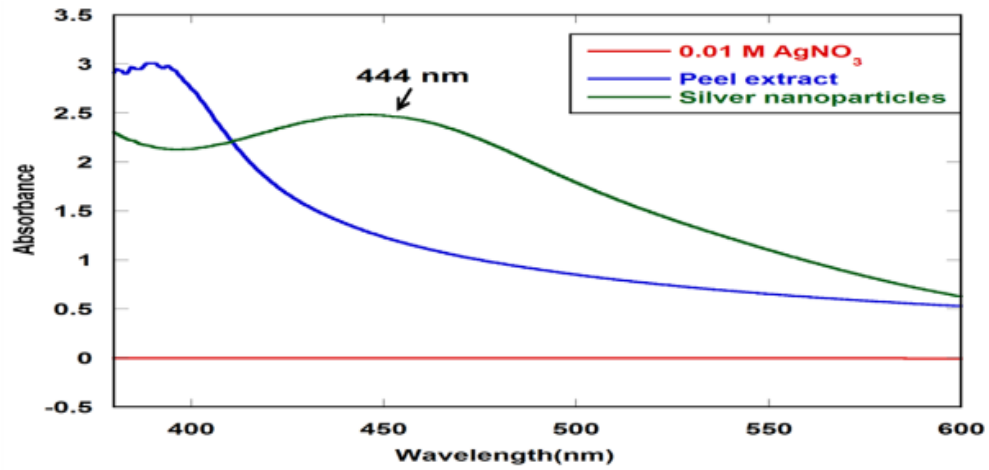

Figure 8. UV-vis absorbance spectra of the synthesized AgNPs using an extract of *C. sinensis* peel

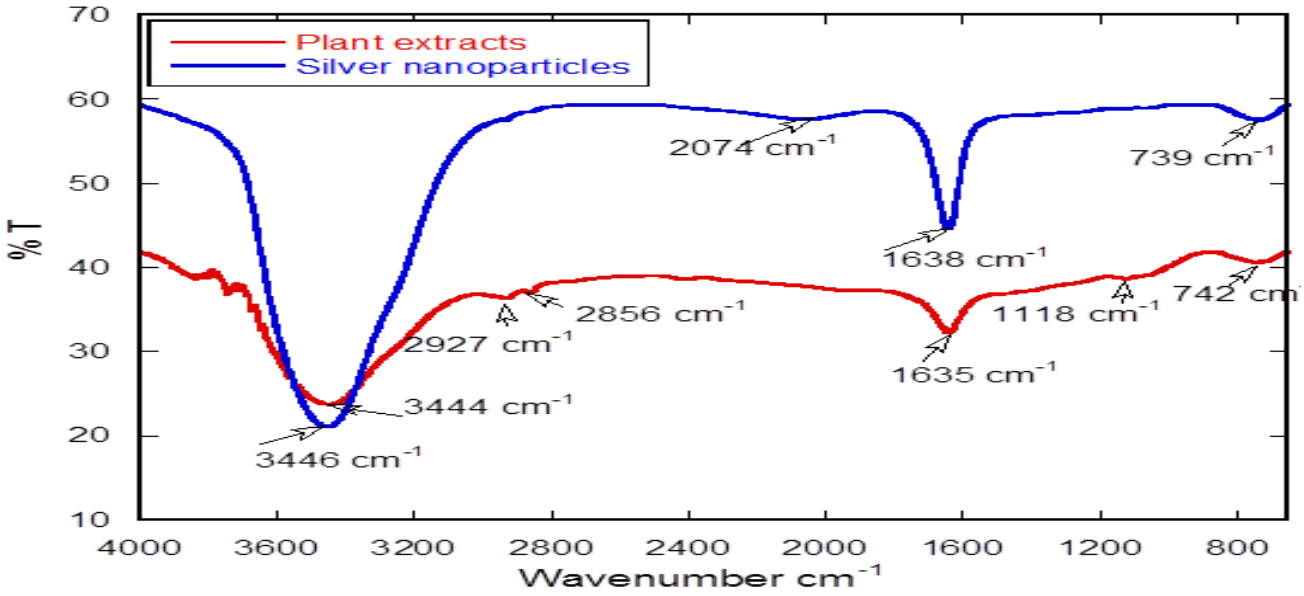

Figure 9. FT-IR spectrum of *C. sinensis* peel extract and synthesized silver nanoparticles

Table 1. Phytochemical test for aqueous peel extract of *Citrus sinensis*

Tested phytochemicals	
Terpenoids	-
Saponins	+
Tannins	+
Flavonoids	+
Alkaloids	+
Steroids	+
Carbohydrates	+

X-ray diffraction

XRD is a very important tool to detect the formation of nanoparticles, confirm the crystal structure and calculate the crystalline nanoparticle size [25]. Figure 10a shows the silver nanoparticles synthesis at 25 °C having three intense peaks were 38.44, 44.3 and 64.82 reprsenting the planes of (111), (200) and (220), respectively which were in good agreement with reference to the unit cell of face centered cubic (FCC) structure of metallic silver (joint committee for powder diffraction standards, JCPDS File No. 04-0783). Figure 10b demonstrates the silver nanoparticles synthesis at 60 °C display three intense peak at 38.42, 44.22 and 64.68 indicating the planes of (111), (200) and (220), respectively. The average size of crystalline silver nanoparticle was calculated from the XRD peaks by using equation 1 [26].

$$D=0.94\lambda/\beta\cos\theta \quad \text{(Eq. 1)}$$

Where, D is the average crystal size, λ is the X-ray wave length and β is the full width at half maximum and θ is the diffraction angle. The average size of synthesized NPs calculated from scherrer formula was found to be 29 nm and 21 nm at 25 °C and at 60 °C, respectively. Also, the XRD result was in agreement with the other earlier researches [27, 28].

Scanning electron microscopy

Scanning electron microscopy is an impotant method for the morphological characterization of synthesized nanomaterials with a high degree of spatial resolution. It has been noticed that the size distribution, size differences and capacity for aggregation depends on experimental conditions, stability of nanoparticles *etc* [29]. Figure 11a, b shows the SEM image of the synthesized silver nanoparticles at 25 °C and 60 °C, respectively. It was found that the nanoparticle formed was spherical in shape with average size 32 nm (17 nm - 45 nm) at 25 °C and 17 nm (10 nm - 37 nm) at 60 °C.

Transmission electron microscopy

The size, shape and morphology of the synthesized silver nanoparticles were determined with the help of transmission electron microscopy. Figure 12a, b shows the TEM images of the AgNPs synthesized at 25 °C and 60 °C temperature, respectively. The AgNPs formed at 25 °C are almost spheroidal in shape with a wide size distribution average size 23 nm (11 nm to 36 nm) and at 60 °C average particle size 16 nm (5 nm to 32 nm). Most of them were spheroidal and decreased for the

higher temperature (60 °C) indicating that raising the reaction temperature leads to AgNPs with narrow size distribution.

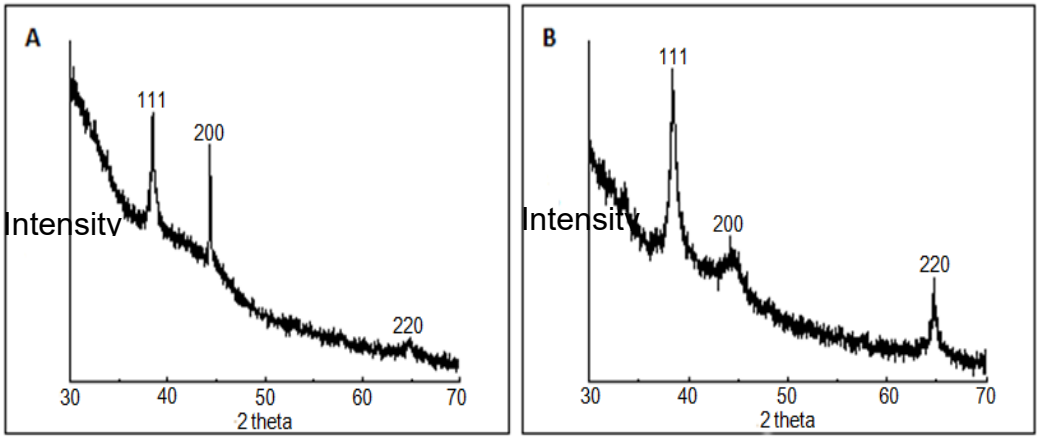

Figure 10. XRD spectra of silver nanoparticles synthesis from *C. sinensis* peel extract at a) 25 °C and b) 60 °C

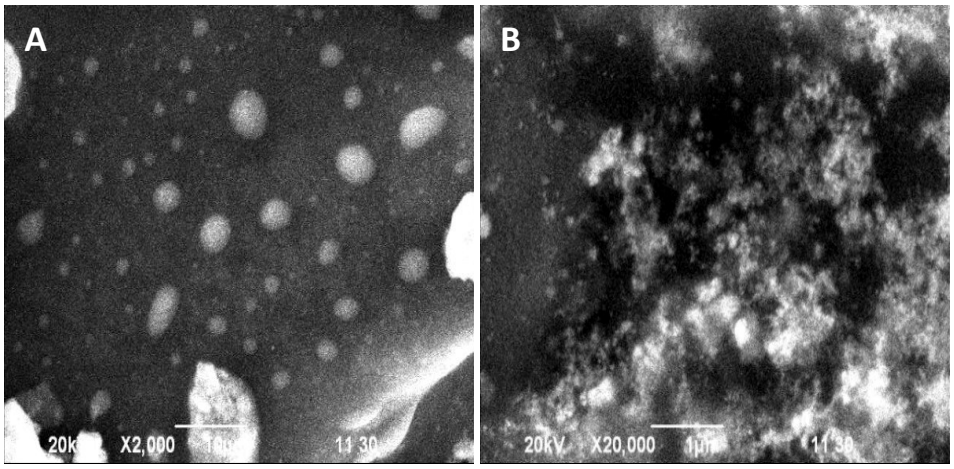

Figure 11. SEM image showing surface morphology of the silver nanoparticles at a) 25 °C and b) 60 °C

Dynamic light scattering

It is used to characterize the size distribution, surface charge and quality of nanoparticles. It is also useful to know the poly dispersity index of AgNPs. The DLS technique uses light to measure the size of particles in a solution. The diameter that is measured in dynamic light scattering is called the hydrodynamic diameter and refers to how a particle diffuses within fluid. PDI measures the homogeneous of nanoparticles. The smaller the PDI the more homogeneous nanoparticles produced. Nanoparticles with PDI value smaller than 0.5 is considered acceptable for drug delivery. It is an

indicator of aggregation in the particles as the value is more it shows a polydisperse system. The hydrodynamic size and PDI value are shown in Table 2.

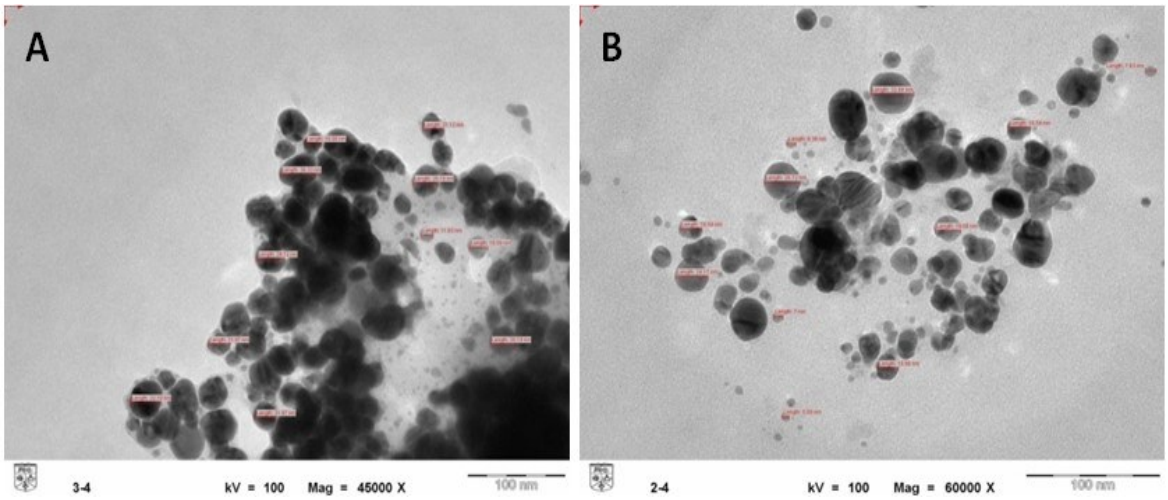

Figure 12. TEM image for silver nanoparticles at (A) 25 °C and (B) 60 °C

Table 2. Size and PDI value for synthesized silver nanoparticle

Synthesized AgNPs	Hydrodynamic size	PDI
at 25 ºC	190 nm	0.371
at 60 ºC	175 nm	0.328

Table 3. Antibacterial activity of tested samples at different doses

Name of bacteria	Zone of inhibition (mm)					
	Peel extracts 40 µg /disc	$AgNO_3$ 40 µg /disc	Antibiotic (tetracycline) 10 µg /disc	AgNPs 30 µg /disc	AgNPs 40 µg /disc	AgNPs 50 µg /disc
E. coli	7 ± 0.5	-	10 ± 1.2	10 ± 0.5	12 ± 1.1	13 ± 0.5
Pseudomonas aeruginosa	9 ± 1.1	-	12 ± 0.4	14 ± 1.2	16 ± 0.5	17 ± 0.7
Bacillus subtilis	8 ± 0.6	-	9 ± 0.5	10 ± 1.0	11 ± 0.6	13 ± 0.4
Staphylococcus aureus	8 ± 1.0	-	11 ± 1.1	8 ± 0.2	10 ± 1.0	12 ± 1.1

Values are given as mean ± S.D. (n = 3)

Antibacterial activity of AgNPs

It was apparent that the synthesized AgNPs showed remarkable inhibition zone against all tested organisms, while aqueous peel extract showed low activity. On the otherhand, 0.01 M $AgNO_3$ did not show any activity against the bacteria (Table 3). The antibiotic tetracycline was used as standard antibacterial agent against tested bacteria. Although AgNPs have been widely used for antimicrobials, their mechanism is still not well understood. Possible antimicrobial mechanisms proposed include (1) interference with cell wall synthesis, (2) inhibition of protein synthesis, (3) interference with nucleic acid synthesis, and (4) inhibition of a metabolic pathway. AgNPs have the ability to increase the permeability of the cell membrane, interfere with DNA replication, denature bacterial proteins, and release silver ions inside the bacterial cell [30]. The power of AgNPs against the tested bacteria was depended up the size and dose. The zone of inhibition increases with the increasing the dose of silver nanoparticles. From the results, it concludes that silver nanoparticles have significant antibacterial activity against *Pseudomonas aeruginosa*, *Escherichia coli* and *Bacillus subtilis* whereas less against *Staphylococcus aureus*.

Conclusions

The green synthesis of silver nanoparticles by using peel extract of *Citrus sinensis* is very simple and eco-friendly method. The separation of this nanoparticle was performed by centrifugation while the identification was done by UV-vis spectra, XRD, FT-IR, SEM, DLS and TEM methods. Reduction of the Ag^+ to Ag^0 during exposure to the *Citrus sinensis* peel extract was followed by color change of the solution from colorless to dark brown. It was observed that surface plasmon resonance peaks for the maximum absorbance of silver nanoparticles occur at 444 nm, indicating that AgNPs were produced. The synthesized AgNPs were subjected to biological evaluation and tested against some bacterial strains. It was found that the AgNPs had moderate to very good bactericidal properties to tested bacteria and therefore represent as a promising antibacterial agent.

Disclosure Statement

No potential conflict of interest was reported by the authors.

References

[1]. Ananda D., Babu S.T.V., Joshi C.G., Shantaram M. *Int. J. Nanomater. Bios.*, 2015, **5**:20

[2]. Ahmed S., Ahmad M., Swami B.L., Ikram S. *J. Adv. Res*., 2016, **7**:17

[3]. Nasseri M.A., Behravesh S., Allahresani A., Kazemnejadi M. *Org. Chem. Res.*, 2019, **5**:190

[4]. Fardood S.T., Ramazani A., Moradnia F., Afsharia Z., Ganjkhanlu S., Zarea F.Y. *Chem. Method.*, 2019, **3**:632

[5]. Borase H.P., Salunke B.K., Salunkhe R.B., Patil C.D., Hallsworth J.E., Kim B.S., Patil S.V. *Appl. Biochem. Biotech*., 2014, **173**:1

[6]. Manthey J.A., Grohmann K. *J. Agric*. *Food Chem*., 2001, **49**:3268

[7]. Terpstra A.H., Lapre J.A., Vries H.T., Beynen A.C. *Eur. J. Nutr*., 2002, **41**:19

[8]. Yang B., Qi F., Tan J., Yu T., Qu C. *Appl. Sci.*, 2019, **9**:2423

[9]. Thi T.U.D., Nguyen T.T., Thi Y.D., Thi K.H.T., Phan B.T., Pham K.N. *RSC Adv*., 2020, **10**:23899

[10]. Skiba M.I., Vorobyova V.I. *Adv. Materials Sci. Eng*., 2019, Article ID 8306015, 8 pages

[11]. Arunachalam R., Dhanasingh S., Kalimuthu B., Uthirappan M., Rose C., Mandal A.B. *Coll. Surfaces B Biointerfaces*, 2012, **94**:226

[12]. Parekh J., Chanda S. *Turk. J. Biotechnol*., 2008, **31**:53

[13]. Guruvaiah P., Arunachalam A., Velan L.P.T. *Asian Pacific J. Tropical Dis*., 2012, **2**:118

[14]. Rakholiya K., Chanda S. *Asian Pac. J. Trop. Biomed*., 2012, **2**:S876

[15]. Mulvaney P. *Langmuir*, 1996, **12**:788

[16]. Mahitha B., Deva P., Raju B., Dillip G.R., Reddy C.M., Mallikarjuna K., Manoj L., Priyanka S., Rao K.J., Sushma N.J. *Dig. J. Nanomat. Biosynth*., 2011, **6**:135

[17]. Ibrahim H.M.M. *J. Radiat. Res. App. Sci.*, 2015, **8**:265

[18]. Zaki S., ElKady M.F., Abd-El-Haleem D. *Mater. Res. Bull*., 2011, **46**:1571

[19]. Srivastava A.A., Kulkarni A.P., Harpale P.M., Zunjarrao R.S. *Int. J. Eng. Sci. Tech*., 2011, **3**:8342

[20]. De Faria A.F., Martinez D.S.T., Meira S.M.M., De Moraes A.C.M., Brandelli A., Filho A.G.S., Alves O.L. *Coll. Surfaces B Biointerfaces*, 2014, **113**:115

[21]. Padalia H., Moteriya P., Chanda S. *Arab. J. Chem*., 2015, **8**:732

[22]. Kokila T., Ramesh P.S., Geetha D. *Appl. Nanosci*., 2015, **5**:911

[23]. Pant G., Nayak N., Prasuna R.G. *Appl. Nanosci*., 2012, **3**:431

[24]. Roopan S.M., Rohit M.G., Rahuman A.A., Kamaraj C., Bharathi A., Surendra T.V. *Ind. Crops. Prod.*, 2013, **43**:631

[25]. Mourdikoudis S., Pallares R.M., Thanh N.T.K. *Nanoscale*, 2018, **10**:12871

[26]. Moradnia F., Taghavi Fardood T., Ramazani A., Gupta V.K. *J. Photochem. Photobiol. A Chem*., 2020, **392**:112433

[27]. Kumar D.A., Kumar V., Palanichamy S.M., Roopan S.M. *Spectrochim. Acta A Mol. Biomol. Spectroscopy*, 2014, **127**:168

[28]. Sivakumar J., Kumar C.P., Santhanam P., Saraswathi N. *Afr. J. Basic Appl. Sci*., 2011, **3**:265

[29]. Fatema S., Shirsat M., Farooqui M., Pathan M.A. *Int. J. Nano Dimens*., 2019, **10**:163

[30]. Guzman M., Dille J., Godet S. *Nanomed.*, 2012, **8**:37

How to cite this manuscript: Kamrun Nahar, Md. Hafezur Rahaman, G.M. Arifuzzaman Khan, Md. Khairul Islam, Sharif Md. Al-Reza*. Green synthesis of silver nanoparticles from *Citrus sinensis* peel extract and its antibacterial potential. *Asian Journal of Green Chemistry*, 5(1) 2021, 135-150. DOI: 10.22034/ajgc.2021.113966